Histol Histopathol (2024) 39: 1053-1063

Histology and Histopathology
From Cell Biology to Tissue Engineering

ORIGINAL ARTICLE Open Access

Expression of the HIF-1α/VEGF pathway is upregulated to protect alveolar bone density reduction in nasal-obstructed rats

Zishan Liu and Yongming Li

Department of Orthodontics, Shanghai Engineering Research Center of Tooth Restoration and Regeneration, School and Hospital of Stomatology, Tongji University, Shanghai, PR China

Summary. Background. Hypoxia and mouth breathing are closely related to maxillofacial bone metabolism and are characteristic of obstructive sleep apnea-hypopnea syndrome (OSAHS). Being key factors in the hypoxia response, hypoxia-inducible factor 1α (HIF-1α) and HIF-responsive gene vascular endothelial growth factor (VEGF) are essential for bone remodeling. This study focuses on the role of the HIF-1α/VEGF pathway in alveolar bone metabolism during OSAHS.

Materials and methods. 36 three-week-old male Wistar rats were divided into three groups: twelve control rats, twelve bilateral nasal obstructed (BNO) rats, twelve BNO rats treated with intraperitoneal injection of Dimethyloxalylglycine (DMOG). After two weeks, the microstructure and bone mineral density (BMD) of alveolar bone were evaluated using micro-computed tomography (micro-CT). The expressions of HIF-1α and VEGF in the alveolar bone were then assessed via immunohistochemistry staining, quantitative real-time polymerase chain reaction (qRT-PCR) and Western blot. Alkaline phosphatase (ALP) staining and Alizarin red S staining were performed to evaluate osteogenesis of bone marrow-derived mesenchymal stem cells (BMSCs).

Results. Significant reductions in alveolar bone density were noted in BNO rats. Bilateral nasal obstruction increased the expressions of HIF-1α and VEGF in alveolar bone. With upregulation of HIF-1α/VEGF via DMOG, alveolar bone density of BNO rats increased. Furthermore, DMOG promoted the osteogenic differentiation of BMSCs by stabilizing the HIF-1α protein and increasing the expression of VEGF.

Conclusion. Bilateral nasal obstruction changes alveolar bone structure and leads to a reduction in alveolar bone density. Moreover, the expression of the HIF-1α/VEGF signaling pathway increases to protect alveolar bone density reduction in BNO rats.

Key words: OSAHS, Hypoxia, HIF-1α/VEGF, Bone density

Corresponding Author: Zishan Liu and Yongming Li, Department of Orthodontics, Shanghai Engineering Research Center of Tooth Restoration and Regeneration, School and Hospital of Stomatology, Tongji University, 399 Middle Yanchang Road, Shanghai 200072, PR China. e-mail: 1727039279@qq.com or 1505427001@qq.com

www.hh.um.es. DOI: 10.14670/HH-18-701

Introduction

Obstructive sleep apnea-hypopnea syndrome (OSAHS) is known to be a disease with high incidence (Peled et al., 2007; Garg et al., 2017; Floras, 2018; Malhotra, 2018). Recent studies have shown that OSAHS incidence is 2-4% in men and 1-2% in women at the average age (Maspero et al., 2015). In addition, bilateral nasal obstruction due to adenoid-tonsil hypertrophy has been suggested to play a critical role in the occurrence of OSAHS (Ant et al., 2017). Adenoid-tonsil hypertrophy has also been found to reduce upper airway volume according to recent studies. Consequently, the body will be in a hypoxic condition, which may lead to severe complications, such as cardiovascular disease (Kukwa et al., 2018; Alqutami et al., 2019; Ramos et al., 2019), maldevelopment of cranial and maxillofacial, and malocclusion. Hypoxia has been shown to cause mandibular growth retardation (Hosomichi et al., 2017) and underdeveloped mandibular ramus/condyles (Lekvijittada et al., 2021) in rats. Mouth breathing is also an important clinical manifestation in patients with OSAHS and is closely related to malocclusion (Emslie et al., 1952). Many researchers have stated that hypoxia and mouth breathing can cause neuromuscular abnormalities in the maxillofacial region (Grippaudo et al., 2016), which may alter maxillofacial development trends and lead to a significantly reduced overbite, increased overjet, and narrower maxillary and shorter mandibular dental arches (Pirilä-Parkkinen et al., 2009). Compared to the general population, patients with

OSAHS have been noted to be more likely to have posterior crossbite, anterior open bite and Class II malocclusion (Souki et al., 2009). In addition to increasing oxygen saturation, treating malocclusion in patients with OSAHS is challenging in orthodontic treatment. Alveolar bone remodeling is affected by various biochemical and mechanical factors (Hadjidakis and Androulakis, 2006) and is the basis of orthodontic tooth movement as the treatment for malocclusion. However, the adaptive structural changes of alveolar bone in patients with OSAHS continues to remain unclear. Understanding changes in alveolar bone metabolism in the OSAHS model is of great significance for treating malocclusion in patients with OSAHS.

Studies have suggested the presence of an association between hypoxia and disorders of bone metabolism, including fracture and mandibular growth retardation. Oxygen serves as an important factor that affects the balance between bone-forming osteoblasts and bone-resorbing osteoclasts. During hypoxia, HIF-1α acts as a transcription factor that combines with HREs (hypoxia response element) in order to induce the expression of target genes. As a HIF-responsive gene, VEGF is essential in angiogenesis and osteogenesis. Numerous studies have already shown that HIF-1α plays an important role during the development, homeostasis, and regeneration of bone mass (Wang et al., 2007; Rauner et al., 2016). Moreover, HIF-1α acts as a regulator in bone-destructive diseases such as osteoarthritis (OA) (Wan et al., 2010). However, the effect of the regulation of HIF-1α on alveolar bone remodeling in patients with OSAHS has yet to be systematically investigated.

In this study, a BNO rat model was constructed in order to simulate the hypoxic environment and mouth breathing of OSAHS, which then explored the structural changes of alveolar bone. Furthermore, the regulation of HIF-1α/VEGF on alveolar bone remodeling and osteogenic differentiation is discussed.

Materials and methods

Animals

3-week-old male Wistar rats were purchased from Sippe-Bk Lab Animal Co (Shanghai, China). All animal experiments were approved by the Animal Ethics Committee of Hubei Experimental Animal Center of Tongji University (NO. Tj-HB-LAC-2021-38). DMOG is a prolyl hydroxylase domain enzyme (PHD) inhibitor that promotes the stabilization of the HIF-1α protein. Rats were randomly divided into three groups: the control group (CON; n=12), BNO group that was treated with an intraperitoneal injection of phosphate buffered saline (PBS, HyClone) (BNO; n=12), and BNO group that was treated with an intraperitoneal injection of DMOG (2 mg qd; MCE, China) (BNO + DMOG; n=12). The rats were then anesthetized with sodium pentobarbital (60 mg/kg) prior to undergoing surgery. The bilateral nostril was then blocked with a portable electric heater for rats in the BNO group. Meanwhile, the surrounding tissues of the bilateral nostrils were burned as control models. DMOG and PBS were given to rats once daily for 14 days since the first day after BNO surgery. Under a 12:12-hour light-dark cycle at a constant temperature room (23-25°C), all rats were raised at the animal center of Tongji University, Shanghai, China. After 14 days, all rats were sacrificed, and their maxillary bone tissues were extracted for analysis.

Micro-CT analysis

The maxillary bone taken from the rats (n=6 each group) were fixed in 4% paraformaldehyde (Sigma-Aldrich, St Louis, MO, USA) for 24h at 4°C. The samples were then scanned using micro-CT (Scanco Medical, Bruttisellen, Switzerland). Next, 20 slices of inter-radicular alveolar bone were measured in the rat maxillary M1 region for 3D reconstruction. Bone volume/tissue ratio (BV/TV, %), bone mineral density (BMD, mg HA/ccm), and trabecular thickness (Tb. Th, mm) were also quantified.

Histological analysis

The samples were fixed in 4% PFA for 24h at 4°C and were then decalcified in 10% EDTA (Sigma-Aldrich) for 8 weeks. Next, the bone samples were embedded in paraffin (SolelyBio, Shanghai, China) and sectioned (5 μm). Hematoxylin and eosin (H&E) staining (Beyotime) was conducted in order to observe the histomorphological characteristics. According to the manufacturer's protocol, alkaline phosphatase (ALP) staining was performed using an ALP assay kit (Nanjing Jiancheng Bioengineering Institute, Nanjing, China).

In regard to immunohistochemistry staining, both HIF-1α (Affinity Biosciences, America) and VEGF (Affinity Biosciences, America) were used at 1:100 dilution. Color development was performed using DAB (Maxim Biotechnology, Fuzhou, China). The slices were then counterstained with methyl green (Sigma), and the sections were finally sealed with neutral balsam. Afterward, the images were captured using a fluorescence microscope (Nikon, Japan). The number of HIF-1α and VEGF positive cells were counted in photographed visual fields (200x magnification). The means of integrated optical density (IOD) of ALP was quantified using ImageJ software.

RNA extraction and quantitative real-time PCR

Total RNA from rat maxillary alveolar bone tissues was purified using Trizol reagent (Takara, Kyoto, Japan). Reverse transcription was carried out using the PrimeScript RT Reagent Kit (Takara, Japan). qRT-PCR was then performed using SYBR Green PCR Master Mix kits on a LightCycler 96 system (Roche, China). All

values were normalized to β-actin. The primers used for qRT-PCR are listed in Table 1.

Western blot

Maxillary alveolar bone tissues were lysed with radioimmunoprecipitation assay (RIPA, Beyotime) buffer containing phenylmethyl sulfonylfluoride (PMSF, Beyotime) and protease/phosphatase inhibitors (Beyotime) for 3h. The total cell protein was lysed with the RIPA buffer containing a protease inhibitor mixture following PBS lavation. The nuclear protein of BMSCs were then extracted according to the protocol of the Nuclear and Cytoplasmic Protein Extraction Kit (Beyotime, Shanghai, China). Each protein sample (50 μg) was separated by sodium dodecyl sulfate-polyacrylamide gel electrophoresis (SDS-PAGE, Epizyme, Shanghai, China) and transferred onto polyvinylidene fluoride membranes (Merck-Millipore, Billerica, MA, USA). The membranes were blocked in 5% bovine serum albumin (BSA, WellBio) for 1h at room temperature, after which they were incubated overnight with primary antibodies: HIF-1α (1:1000, Affinity, Jiangsu, China), β-actin (1:3000, Affinity, Jiangsu, China), VEGF (1:1000, Affinity, Jiangsu, China), LaminB1 (1:1000, Affinity, Jiangsu, China), Runx2 (1:1000, Affinity, Jiangsu, China), COL I (1:1000, Affinity, Jiangsu, China), ALP (1:1000, Boster, Hubei, China), OCN (1:1000, Boster, Hubei, China). After washing with TBST buffer 3 times, the membranes were labelled with a secondary antibody for another 1h at room temperature. The Odyssey CLx imaging system was then utilized in order to scan the bands. The relative protein expression was standardized to β-actin and quantified with ImageJ software.

Isolation and culture of BMSCs

The femurs and tibias of 3-week-old Wistar rats were flushed to acquire bone marrow. Next, bone marrow clumps were broken up using an 18-gauge sterile needle. Cells were then cultured in complete α-MEM containing 10% fetal bovine serum (FBS) and 1% penicillin/streptomycin at 37°C under 5% CO_2. The culture medium was replaced every 3 days. When the cells attained approximately 80% confluence, the cells were passaged at 1:3. BMSCs were used between three to five passages.

Cell counting kit-8 (CCK-8) assay

The CCK-8 assay (Beyotime, China) was utilized to evaluate the different concentrations of DMOG on cell viability. BMSCs were cultured in 96-well plates at 1000 cells/mL in 100 μL of complete α-MEM. Then, increasing concentrations of DMOG (0, 100, 500, 1000, 2000 μM) were added to cells for 48h. After being incubated with 10 μL/well of CCK-8 reagent for 2h, the optical density was measured at 450 nm. Cell viability was subsequently quantified relative to the untreated controls.

ALP Staining and quantitative analysis

ALP staining was performed using a BCIP/NBT Alkaline Phosphatase Color Development Kit (Beyotime). Following 7 days of osteogenic induction with 500μM DMOG, the cells were fixed with 4% PFA (Sigma) for 30 min. The cells were then mixed with BCIP/NBT staining solution for 30 min at room temperature in the dark. Digital images were taken using a Canon Single Lens Reflex camera and were quantified with ImageJ.

Alizarin Red S staining

Following 21 days of osteogenic induction with 500μM DMOG, the cells were fixed with 4% PFA (Sigma) for 30 min. After washing with PBS three times, the cells were stained with 1% alizarin red S (Solarbio, Beijing, China) for 5 min. Then, the dye liquor was washed off, and pictures were taken using a light microscope (Nikon, Japan) under 100x magnification, which were then quantified using the ImageJ software.

Statistical analysis

Statistical analysis was conducted using GraphPad Prism 8.0 and SPSS 20.0. The data were expressed as the mean ± SEM. Comparisons between groups were analyzed using one-way analysis of variance (ANOVA) and then, the Bonferroni post hoc test was used to test the selected comparison or Dunnett's multiple comparison post hoc test, if each group needed to be

Table 1. The primers used for qRT-PCR.

Gene	Forward (5'-3')	Reverse (5'-3')
β-Actin	CATCCGTAAAGACCTCTATGCCAAC	ATGGAGCCACCGATCCACA
VEGF	AGGAGGGCAGAATCATCACG	CAAGGCCCACAGGGATTTTCT
HIF-1α	ACTTGGCAACCTTGGATTGGA	GCACCAAGCAGGTCATAGGT
ALP	TATGTCTGGAACCGCACTGAAC	CACTAGCAAGAAGAAGCCTTTGG
OCN	CAGACAAGTCCCACACAGCA	CCAGCAGAGTGAGCAGAGAGA
RUNX2	ACTTCCTGTGCTCGGTGCT	GACGGTTATGGTCAAGGTGAA
COL I	GCTCCTCTTAGGGGCCACT	ATTGGGGACCCTTAGGCCAT

compared with the control group. A value of $P<0.05$ was considered to be statistically significant.

Results

Alveolar bone density was found to be reduced in BNO groups, which was impaired by the HIF1-α stabilizer.

The 3D reconstruction demonstrated obvious alveolar bone density reduction in the BNO group compared with the CON group. In order to explore the effect of HIF-1α on alveolar bone structure, the effect of DMOG intraperitoneal injection in the BNO model group was examined. The corresponding analysis showed that alveolar bone density at the root furcation of the first molar of the maxillae was promoted in the BNO+DMOG group compared with the BNO group. In addition, the micro-CT analyses indicated synchronous change in BV/TV and Tb.Th in the alveolar bone (Fig. 1A,B).

HIF1-α and VEGF expressions in the alveolar bone of BNO groups were elevated and were further enhanced by the HIF1-α stabilizer.

Expressions of HIF-1α and VEGF in alveolar bone were examined via immunohistochemistry at the root furcation of the first molar of maxillae. The findings showed that more HIF-1α-positive and VEGF-positive points were observed in the BNO group compared to the control group. Moreover, the difference was noted to be larger following treatment with DMOG. A semiquantitative analysis revealed a noticeable rise of HIF-1α and VEGF appearance in the BNO+DMOG group after 14 days compared with the BNO group (Figs. 2A, 3A). In order to further illustrate the role of

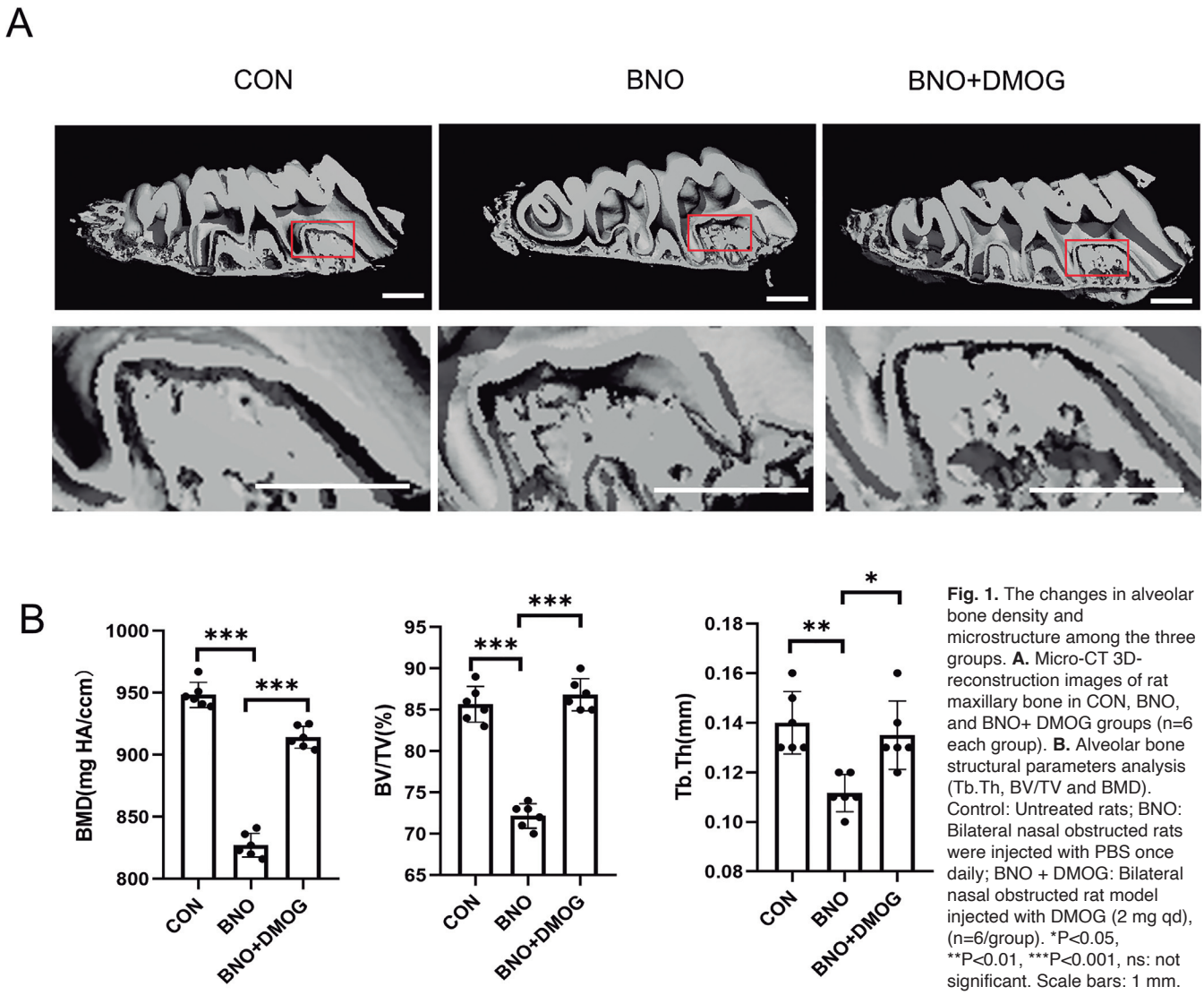

Fig. 1. The changes in alveolar bone density and microstructure among the three groups. **A.** Micro-CT 3D-reconstruction images of rat maxillary bone in CON, BNO, and BNO+ DMOG groups (n=6 each group). **B.** Alveolar bone structural parameters analysis (Tb.Th, BV/TV and BMD). Control: Untreated rats; BNO: Bilateral nasal obstructed rats were injected with PBS once daily; BNO + DMOG: Bilateral nasal obstructed rat model injected with DMOG (2 mg qd), (n=6/group). *P<0.05, **P<0.01, ***P<0.001, ns: not significant. Scale bars: 1 mm.

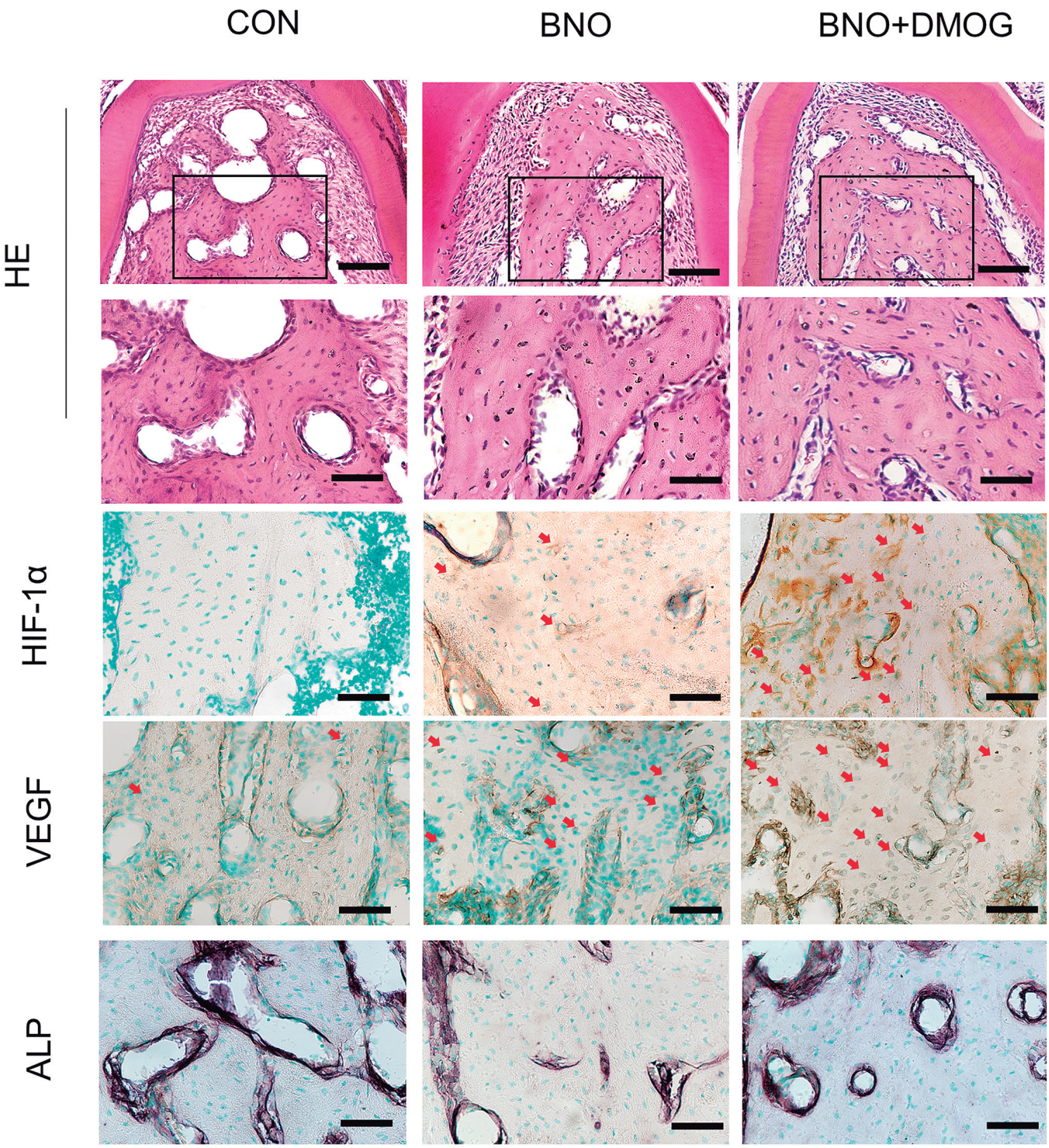

Fig. 2. The expressions of HIF-1α and VEGF in alveolar bone via IHC staining. H&E staining for the inter-radicular alveolar bone in the three groups. Boxed area is shown in detail. IHC staining of rat maxillary alveolar bone for HIF-1α, VEGF. The red arrows represent HIF-1α + and VEGF+ cells. Representative ALP staining images of each group. Control: Untreated rats; BNO: Bilateral nasal obstructed rats were injected with PBS once daily; BNO + DMOG: Bilateral nasal obstructed rat model injected with DMOG (2 mg qd), (n=6/group). *p<0.05, **p<0.01, ***p<0.001, ns: not significant. Scale bars: H&E 50 and 25 μm; IHC, 25 μm.

HIF-1α and VEGF during bone metabolism, qRT-PCR and Western blot analysis of the rat maxillary alveolar bone were carried out. In the BNO group, mRNA levels of HIF-1α and VEGF were found to be increased compared with those in the control groups. In the BNO+DMOG group, the mRNA levels of VEGF were noted to be increased compared with those in the BNO groups (Fig. 3B). The expression of HIF-1α at the mRNA level was not found to be significantly different compared to the BNO group, which was caused by the action principle of DMOG. Western blot analysis showed that the protein levels of HIF-1α and VEGF rose in the BNO groups compared with those in the control groups. Moreover, in the BNO+DMOG groups, the protein levels of HIF-1α and VEGF were shown to be further increased (Fig. 3C,D). ALP staining of alveolar bone also showed that the osteogenesis of BNO alveolar bone was less than that of the control group, which was enhanced following injection of DMOG (Figs. 2A, 3A).

Effects of HIF1-α stabilizer on cell Viability

In order to observe the effects of dimethyl-oxalylglycine (DMOG) on cell viability in BMSCs, BMSCs were cultured with different concentrations (0, 100, 500, 1000, 2000 μM) of DMOG for 48h. The results showed that 1 mM ($P<0.05$) and 2 mM ($P<0.05$) of DMOG inhibited BMSC proliferation (Fig. 4A). Accordingly, 500μM DMOG was selected as optimal concentrations for the follow-up experiments.

The osteogenic potential in BMSCs was enhanced via activation of the HIF-1α/VEGF signaling pathway.

Since DMOG can effectively promote nuclear accumulation of HIF-1α, the relative intranuclear and extranuclear HIF-1α protein levels were detected in BMSCs, which was stimulated with 500 μM DMOG for 30, 60 and 90 min (Fig. 4B). Intranuclear HIF-1α protein expression levels were found to be considerably elevated while extracellular expression levels declined, indicating that HIF-1α transferred into the nucleus. BMSCs treated with DMOG for 12h exhibited increased VEGF gene and protein expression levels (Fig. 4C,D). Since DMOG was observed to enhance HIF-1α/VEGF signaling pathway activation, in order to examine osteogenic differentiation, the mRNA expression of the osteogenic markers' ALP in BMSCs treated with or without 500μM DMOG was first assessed. The quantitative real-time results demonstrated that compared with the control groups, the expression of ALP was increased by DMOG in a dose-dependent manner (Fig. 5A), especially at 500 μM. Then, the expression of the osteogenic markers (ALP, RUNX2, COL I, OCN) at the gene and protein levels following a 48h culture treated with or without 500 μM DMOG was assessed. Here, DMOG treatment in BMSCs for 48h was shown to lead to significant increases in osteogenic markers mRNA and protein expression compared with the control groups (Fig. 5B,C). In order to evaluate the differentiation potential of the BMSCs, ALP staining and Alizarin Red S staining

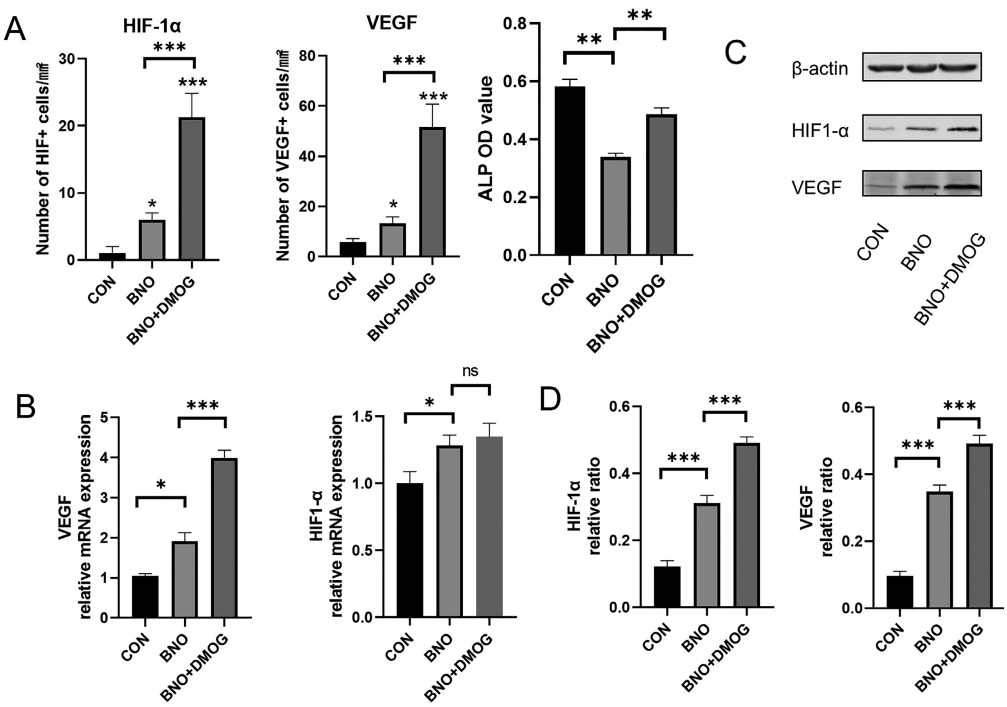

Fig. 3. The expressions of HIF-1α and VEGF in alveolar bone. **A.** Quantification of VEGF+ and HIF-1α + cells in the alveolar bone. The means of the integrated optical density (IOD) of ALP. **B.** Levels of HIF-1α and VEGF were measured by qRT-PCR in the three groups. **C.** The representative Western blotting bands of HIF-1α, VEGF protein. **D.** The quantification of HIF-1α, VEGF protein. Band densities were assessed as fold changes relative to the β-actin control. Control: Untreated rats; BNO: Bilateral nasal obstructed rats were injected with PBS once daily; BNO + DMOG: Bilateral nasal obstructed rat model injected with DMOG (2 mg qd), (n=6/group). *P<0.05, **P<0.01, ***P<0.001, ns: not significant.

were performed after 7-day and 21-day osteogenic induction, respectively. Accordingly, DMOG treatment yielded stronger ALP and Alizarin Red S staining (Fig. 5D,E). Thus, the osteogenic differentiation of BMSCs can be promoted by activating the HIF-1α/VEGF signaling pathway.

Discussion

OSAHS is commonly encountered in clinical practice and has high incidence, which may also lead to malocclusion. Accordingly, studying alveolar bone structure changes for the treatment of malocclusion in patients with OSAHS is vital. In this study, alveolar bone density at the root furcation of the first molar of maxillae was found to be reduced in rats with BNO. Meanwhile, the expressions of HIF-1α and VEGF in protein and mRNA levels were found to be increased in BNO rat model alveolar bone. In order to explore the function of HIF-1α and VEGF in alveolar bone density loss due to bilateral nasal obstruction, the expression of HIF-1α in rats with BNO was further upregulated. According to the observed findings, alveolar bone density increased compared to the BNO rat model. Moreover, upregulating the expression of HIF-1α and VEGF was shown to promote the osteogenic differentiation of BMSCs. Accordingly, it was shown that an increase in the HIF-1α/VEGF signal pathway

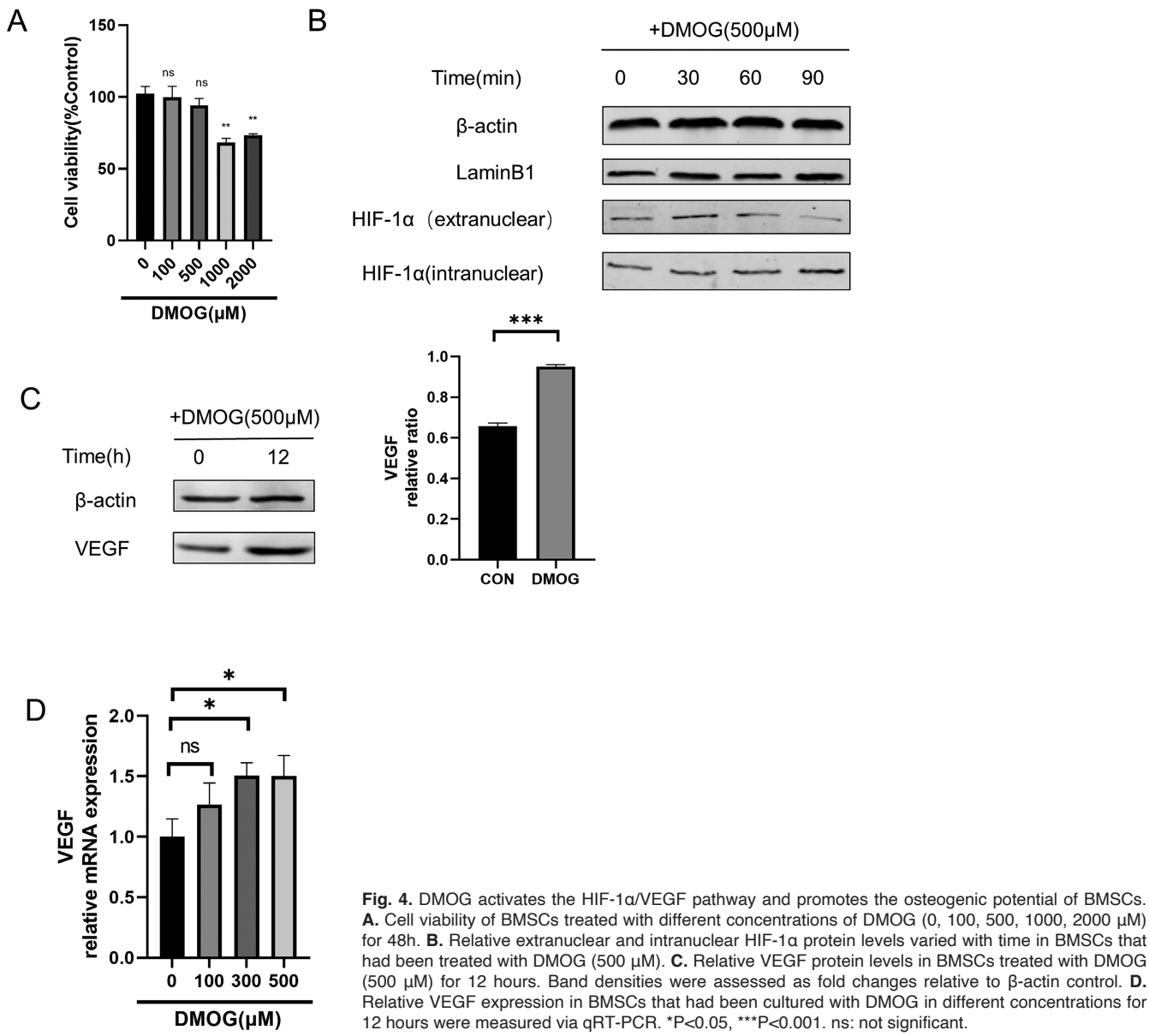

Fig. 4. DMOG activates the HIF-1α/VEGF pathway and promotes the osteogenic potential of BMSCs. **A.** Cell viability of BMSCs treated with different concentrations of DMOG (0, 100, 500, 1000, 2000 μM) for 48h. **B.** Relative extranuclear and intranuclear HIF-1α protein levels varied with time in BMSCs that had been treated with DMOG (500 μM). **C.** Relative VEGF protein levels in BMSCs treated with DMOG (500 μM) for 12 hours. Band densities were assessed as fold changes relative to β-actin control. **D.** Relative VEGF expression in BMSCs that had been cultured with DMOG in different concentrations for 12 hours were measured via qRT-PCR. *P<0.05, ***P<0.001. ns: not significant.

could facilitate osteogenic differentiation and enhance bone formation in BNO rats.

The results of this study indicate that bilateral nasal obstruction leads to a decrease in bone density, trabecular bone volume fraction, and trabecular thickness in the maxillary alveolar bones of Wistar rats. These findings may be related to hypoxia, oral breathing and sleep disturbances due to bilateral nasal obstruction. Because of nasal obstruction, rats were located in a hypoxic environment where their physiological activities

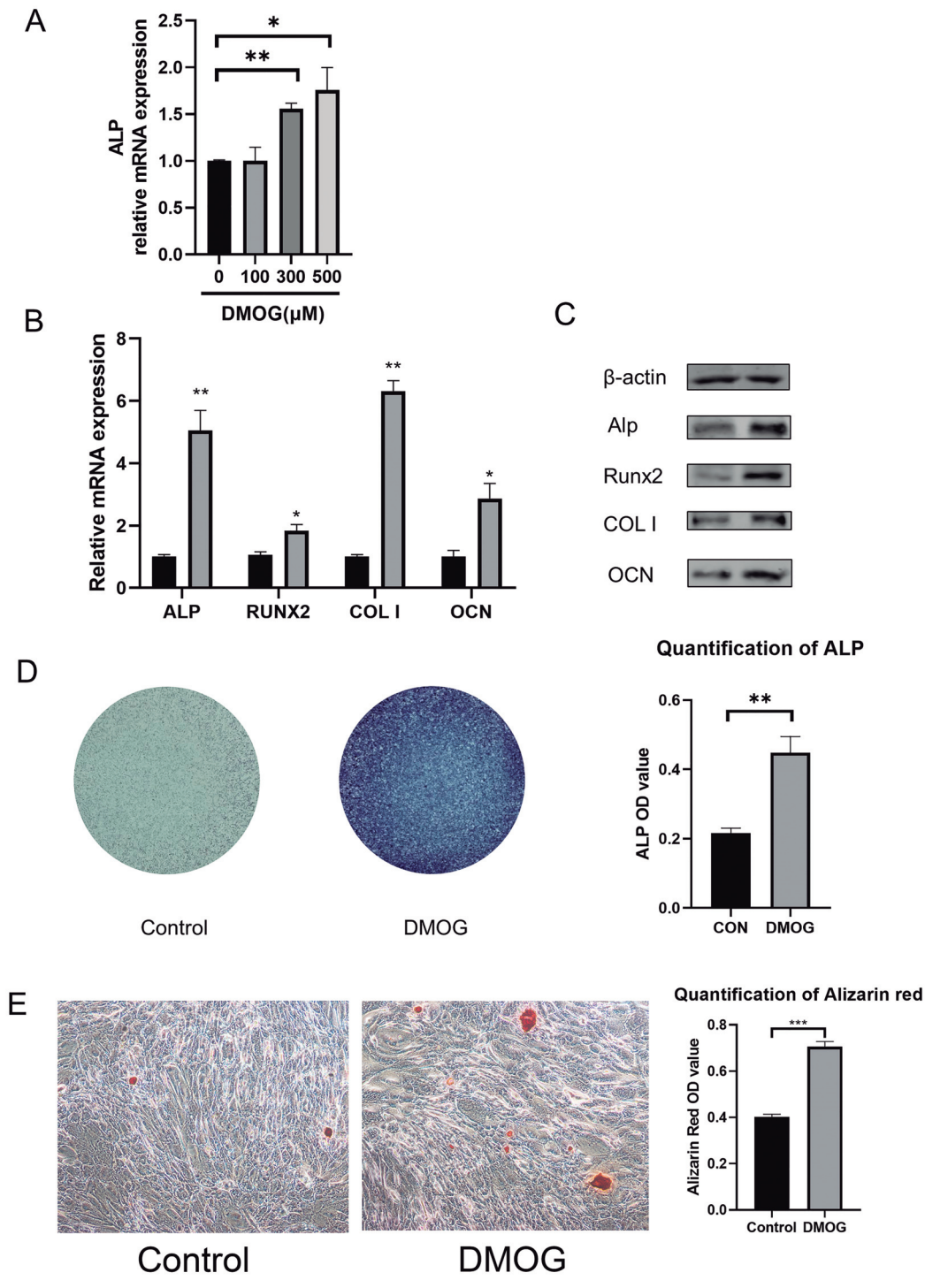

Fig. 5. DMOG promotes the osteogenic potential of BMSCs. **A.** Relative ALP expression in BMSCs cultured with DMOG in different concentrations for 48h were measured via qRT-PCR. **B.** Relative osteogenic marker (ALP, RUNX2, COL I, OCN) mRNA expression in BMSCs cultured with DMOG in 500 μM for 48h were measured via qRT-PCR. **C.** Relative osteogenic marker (ALP, RUNX2, COL I, OCN) protein levels in BMSCs treated with DMOG (500 μM) for 48h. Band densities were assessed as fold changes relative to β-actin control. **D.** ALP staining results in two groups and the optical density analysis after 7 days of osteogenic induction. **E.** Alizarin Red S staining results in two groups and the optical density analysis after 21 days of osteogenic induction (100X magnification), (n=3/group). *p<0.05, **p<0.01, ***p<0.001. ns: not significant.

were inhibited. Previous studies have shown that osteogenesis and osteoblast matrix mineralization is inhibited in rat osteoblasts because of decreased osteoblast proliferation in a hypoxic environment (Utting et al., 2006). The acidosis and oxidative stress induced by hypoxia are known to be harmful to bones. Specifically, acidosis activates osteoclasts and inhibits mineral deposition by osteoblasts (Arnett, 2010). Oxidative stress is related to osteoclast stimulation and inhabitation of osteoblast differentiation (Amstrup et al., 2013). BNO rats carry out breathing from their mouths throughout the day, and one study reported that decreased chewing activity was noted during mouth breathing (Hsu and Yamaguchi, 2012). To a certain extent, the reduction of chewing activity will affect alveolar bone remodeling by reducing stress stimulation. Sleep disturbances can affect the sympathetic tone by regulating the secretion rhythm of leptin and melatonin, leading to decreased bone mass (Satomura et al., 2007; Yadav and Karsenty, 2009; Pan and Kastin, 2014). In conclusion, further research on the mechanism of decreased alveolar bone mineral density should be performed.

HIF-1 (hypoxia-inducible factor 1) consists of the HIF-1α and β subunits and is a key transcription factor of oxygen balance, playing an essential role in maintaining oxygen supply (Semenza, 1998, 1999). In the normoxic state, HIF-1α has been shown to be hydroxylated by prolyl hydroxylase domain enzymes (PHD), which are then degraded by proteasomal. In order to maintain normal bodily activities, HIF-1α is not degraded and acts as a transcription factor to induce the expression of target genes during hypoxia (Kallio et al., 1998) such as VEGF (Maes et al., 2021). Researchers have reported that during bone homeostasis, osteoblast-derived VEGF can induce angiogenic effects by working on adjacent endothelial cells (ECs) (Hoeben et al., 2004; Coultas et al., 2005). Moreover, VEGF has been shown to be released from osteoblastic cells in order to regulate osteoblast differentiation and mineralization by an autocrine mechanism (Thi et al., 2010; Liu et al., 2012). In this study, the expression of HIF-1α and VEGF was found to increase at the gene and protein levels in BNO rats. DMOG is a PHD inhibitor that can promote the nuclear accumulation of HIF-1α and enable its association with HIF-1β (hypoxia-inducible factor 1β) as well as other factors. In order to explore the role of HIF-1α, DMOG was used to stabilize HIF-1α protein in rats with BNO. The results indicated that with the HIF-1α protein stabilized, the expression of VEGF at the gene and protein levels are enhanced, and the reduction of alveolar bone density is suppressed. To further investigate the effect of HIF-1α and VEGF on the osteogenic differentiation ability of osteoblast precursor cells, rat BMSC cells were extracted. *In vitro*, DMOG was used to stimulate the nuclear accumulation of HIF1-α in BMSCs, in which osteogenic differentiation was shown to be enhanced with a rise in HIF-1α and VEGF expression in BMSCs. The corresponding results indicated that the expression of the HIF-1α/VEGF signaling pathway is upregulated in order to promote bone formation and protect alveolar bone density reduction in BNO rats.

Although the upregulation of HIF-1α and VEGF was observed to promote bone formation to a certain extent, it did not play a dominant role in the regulation of bone metabolism during hypoxia. Hypoxia is a complicated condition that appears to be a key mediator of bone metabolism and may be associated with abnormal bone health, which is accompanied by the stimulation of glycolysis, hypoxic pathways, ROS, downstream effects, and acidosis (Arnett, 2010; Jelkmann, 2011; Zepeda et al., 2013). Bone metabolism is dependent on hypoxic exposure levels (Basu et al., 2013; O'Brien et al., 2018), time (Rittweger et al., 2016) and frequency (Guner et al., 2013). A variety of animal models can simulate OSAHS. In this study, bilateral nasal obstruction modeling was adopted to simulate the two main features of respiratory obstruction and oral respiration. One limitation of this study was that it was not simulated only at night, which needs further refining. Moreover, this study was limited to rats and may not be applicable to humans.

Overall, this study provided evidence on alveolar bone density reduction and increased expression of HIF-1α and VEGF in bilateral nasal obstructed rats. *In vitro*, the upregulation of the HIF-1α/VEGF signaling pathway was shown to promote the osteogenic differentiation of BMSCs. *In vivo*, the expression of HIF-1α/VEGF signaling pathway was found to be upregulated in order to protect alveolar bone density reduction in BNO rats. Furthermore, this study illustrated a possible role of HIF-1α/VEGF signaling in osteogenic differentiation of precursor cells and hypoxia-mediated bone metabolism. This study has innovatively established the status of BNO rats as simulators of OSAHS patients and explored the situation of alveolar bone remodeling. However, there is a lack of sufficient clinical data on bone remodeling in OSAHS patients, indicating a promising future direction for further studies.

Funding. This work was supported by the National Natural Science Foundation of China (Program Nos. 81970921).

Data Availability. The datasets used and/or analyzed during the current study are available from the corresponding author upon request.

Conflicts of Interest. The authors declare that they have no competing interests.

Authors' Contributions. ZL and YL designed the study. ZL conducted the experiments and wrote the manuscript. YL revised the manuscript. All authors have read and approved the manuscript.

References

Alqutami J., Elger W., Grafe N., Hiemisch A., Kiess W. and Hirsch C. (2019). Dental health, halitosis and mouth breathing in 10-to-15 year old children: A potential connection. Eur. J. Paediatr. Dent. 20, 274-279.

Amstrup A.K., Sikjaer T., Mosekilde L. and Rejnmark L. (2013).

Melatonin and the skeleton. Osteoporos. Int. 24, 2919-2927.

Ant A., Kemaloglu Y.K., Yilmaz M. and Dilci A. (2017). Craniofacial deviations in the children with nasal obstruction. J. Craniofac. Surg. 28, 625-628.

Arnett T.R. (2010). Acidosis, hypoxia and bone. Arch. Biochem. Biophys. 503, 103-109.

Basu M., Malhotra A.S., Pal K., Chatterjee T., Ghosh D., Haldar K., Verma S.K., Kumar S., Sharma Y.K. and Sawhney R.C. (2013). Determination of bone mass using multisite quantitative ultrasound and biochemical markers of bone turnover during residency at extreme altitude: a longitudinal study. High Alt. Med. Biol. 14, 150-154.

Coultas L., Chawengsaksophak K. and Rossant J. (2005). Endothelial cells and VEGF in vascular development. Nature 438, 937-945.

Emslie R.D., Massler M. and Zwemer J.D. (1952). Mouth breathing. I. Etiology and effects; a review. J. Am. Dent. Assoc. 44, 506-21.

Floras J.S. (2018). Sleep apnea and cardiovascular disease: An enigmatic risk factor. Circ. Res. 122, 1741-1764.

Garg R.K., Afifi A.M., Garland C.B., Sanchez R. and Mount D.L. (2017). Pediatric obstructive sleep apnea: Consensus, controversy, and craniofacial considerations. Plast. Reconstr. Surg. 140, 987-997.

Grippaudo C., Paolantonio E.G., Antonini G., Saulle R., La Torre G. and Deli R. (2016). Association between oral habits, mouth breathing and malocclusion. Acta Otorhinolaryngol. Ital. 36, 386-394.

Guner I., Uzun D.D., Yaman M.O., Genc H., Gelisgen R., Korkmaz G.G., Hallac M., Yelmen N., Sahin G., Karter Y. and Simsek G. (2013). The effect of chronic long-term intermittent hypobaric hypoxia on bone mineral density in rats: role of nitric oxide. Biol. Trace Elem. Res. 154, 262-267.

Hadjidakis D.J. and Androulakis I.I. (2006). Bone remodeling. Ann. NY Acad. Sci. 1092, 385-396.

Hoeben A., Landuyt B., Highley M.S., Wildiers H., Van Oosterom A.T. and De Brujin E.A. (2004). Vascular endothelial growth factor and angiogenesis. Pharmacol. Rev. 56, 549-580.

Hosomichi J., Kuma Y.-I., Oishi S., Nagai H., Maeda H., Usumi-Fujita R., Shimizu Y., Kaneko S., Shitano C., Suzuki J.-I., Yoshida K.-I. and Ono T. (2017). Intermittent hypoxia causes mandibular growth retardation and macroglossia in growing rats. Am. J. Orthod. Dentofacial Orthop. 151, 363-371.

Hsu H.Y. and Yamaguchi K. (2012). Decreased chewing activity during mouth breathing. J. Oral Rehabil. 39, 559-567.

Jelkmann W. (2011). Regulation of erythropoietin production. J. Physiol. 589, 1251-1258.

Kallio P.J., Okamoto K., O'Brien S., Carrero P., Makino Y., Tanaka H. and Poellinger L. (1998). Signal transduction in hypoxic cells: inducible nuclear translocation and recruitment of the CBP/p300 coactivator by the hypoxia-inducible factor-1alpha. EMBO J. 17, 6573-6586.

Kukwa W., Guilleminault C., Tomaszewska M., Kukwa A., Krzeski A. and Migacz E. (2018). Prevalence of upper respiratory tract infections in habitually snoring and mouth breathing children. Int. J. Pediatr. Otorhinolaryngol. 107, 37-41.

Lekvijittada K., Hosomichi J., Maeda H., Hong H., Changsiripun C., Kuma Y.-I., Oishi S., Suzuki J.-I., Yoshida K.-I. and Ono T. (2021). Intermittent hypoxia inhibits mandibular cartilage growth with reduced TGF-β and SOX9 expressions in neonatal rats. Sci. Rep. 11, 1140.

Liu Y., Berendsen A.D., Jia S., Lotinun S., Baron R., Ferrara N. and Olsen B.R. (2012). Intracellular VEGF regulates the balance between osteoblast and adipocyte differentiation. J. Clin. Invest. 122, 3101-3113.

Maes C., Carmeliet G. and Schipani E. (2021). Hypoxia-driven pathways in bone development, regeneration and disease. Nat. Rev. Rheumatol. 8, 358-366.

Malhotra R.K. (2018). Neurodegenerative disorders and sleep. Sleep Med. Clin. 13, 63-70.

Maspero C., Giannini L., Galbiati G., Rosso G. and Farronato G. (2015). Obstructive sleep apnea syndrome: a literature review. Minerva Stomatol. 64, 97-109.

O'Brien K.A., Pollock R.D., Stroud M., Lambert R.J., Kumar A., Atkinson R.A., Green D.A., Anton-Solanas A., Edwards L.M. and Harridge S.D.R. (2018). Human physiological and metabolic responses to an attempted winter crossing of Antarctica: the effects of prolonged hypobaric hypoxia. Physiol. Rep. 6, e13613.

Pan W. and Kastin A.J. (2014). Leptin: a biomarker for sleep disorders? Sleep Med. Rev. 18, 283-290.

Peled N., Kassirer M., Shitrit D., Kogan Y., Shlomi D., Berliner A.S. and Kramer M.R. (2007). The association of OSA with insulin resistance, inflammation and metabolic syndrome. Respir. Med. 101, 1696-1701.

Pirilä-Parkkinen K., Pirttiniemi P., Nieminen P., Tolonen U., Pelttari U. And Löppönen H. (2009). Dental arch morphology in children with sleep-disordered breathing. Eur. J. Orthod. 31, 160-167.

Ramos V.M., Nader C.M., Meira Z.M., Capanema F.D., Franco L.P., Tinano M.M., Anjos C.P., Nunes F.B., Oliveira I.S., Guimarães R.E. and Becker H.M.G. (2019). Impact of adenotonsilectomy on nasal airflow and pulmonary blood pressure in mouth breathing children. Int. J. Pediatr. Otorhinolaryngol. 125, 82-86.

Rauner M., Franke K., Murray M., Singh R.P., Hiram-Bab S., Platzbecker U., Gassmann M., Socolovsky M., Neumann D., Gabet Y., Chavakis T., Hofbauer L.C. and Ben Wielockx B. (2016). Increased EPO levels are associated with bone loss in mice lacking PHD2 in EPO-producing cells. J. Bone Miner. Res. 31, 1877-1887.

Rittweger J., Debevec T., Frings-Meuthen P., Lau P., Mittag U., Ganse B., Ferstl P.G., Simpson E.J., Macdonald I.A., Eiken O. and Mekjavic I.B. (2016). On the combined effects of normobaric hypoxia and bed rest upon bone and mineral metabolism: Results from the PlanHab study. Bone 91, 130-138.

Satomura K., Tobiume S., Tokuyama R., Yamasaki Y., Kudoh K., Maeda E. and Nagayama M. (2007). Melatonin at pharmacological doses enhances human osteoblastic differentiation *in vitro* and promotes mouse cortical bone formation *in vivo*. J. Pineal Res. 42, 231-239.

Semenza G.L. (1998). Hypoxia-inducible factor 1: master regulator of O_2 homeostasis. Curr. Opin. Genet. Dev. 8, 588-594.

Semenza G.L. (1999). Regulation of mammalian O_2 homeostasis by hypoxia-inducible factor 1. Annu. Rev. Cell Dev. Biol. 15, 551-578.

Souki B.Q., Pimenta G.B., Souki M.Q., Franco L.P., Becker H.M.G. and Pinto J.A. (2009). Prevalence of malocclusion among mouth breathing children: do expectations meet reality? Int. J. Pediatr. Otorhinolaryngol. 73, 767-773.

Thi M.M., Suadicani S.O. and Spray D.C. (2010). Fluid flow-induced soluble vascular endothelial growth factor isoforms regulate actin adaptation in osteoblasts. J. Biol. Chem. 285, 30931-30941.

Utting J.C., Robins S.P., Brandao-Burch A., Orriss I.R., Behar J. and Arnett T.R. (2006). Hypoxia inhibits the growth, differentiation and bone-forming capacity of rat osteoblasts. Exp. Cell Res. 312, 1693-1702.

Wan C., Shao J., Gilbert S.R., Riddle R.C., Long F., Johnson R.S., Schipani E. and Clemens T.L. (2010). Role of HIF-1alpha in skeletal development. Ann. NY Acad. Sci. 1192, 322-326.

Wang Y., Wan C., Deng L., Liu X., Cao X., Gilbert S.R., Bouxsein M.L., Faugere M.-C., Guldberg R.E., Gerstenfeld L.C., Haase V.H., Johnson R.S., Schipani E. and Clemens T.L. (2007). The hypoxia-inducible factor alpha pathway couples angiogenesis to osteogenesis during skeletal development. J. Clin. Invest. 117, 1616-1626.

Yadav V.K. and Karsenty G. (2009). Leptin-dependent co-regulation of bone and energy metabolism. Aging (Albany NY), 1, 954-956.

Zepeda A.B., Pessoa Jr A., Castillo R.L., Figueroa C.A., Pulgar V.M. and Farías J.G. (2013). Cellular and molecular mechanisms in the hypoxic tissue: role of HIF-1 and ROS. Cell Biochem. Funct. 31, 451-459.

Accepted January 2, 2024